

Supplemental Material (Snow et al.)

Case Presentations

Patients 1-4 and 6-8 and selected relatives were evaluated at Cincinnati Children's Hospital Medical Center. Patient 5 was originally evaluated at Dana Farber Cancer Institute, in consult with Dr. Nichols at Children's Hospital of Philadelphia. Informed consent was provided by the families according to an Institutional Review Board (IRB)-approved research protocol. All healthy control subjects were studied according to IRB-approved protocols.

Case 1: Patient 1 (Pt1) originally presented at 3 years of age with a history of failure to thrive, emesis, and abdominal pain. Evaluation revealed a non-metastatic, extranodal diffuse large B-cell lymphoma involving the GI tract. He achieved complete remission with standard-of-care chemotherapy. At 7 years of age, routine follow-up imaging revealed another abdominal mass, consistent with non-metastatic, extranodal diffuse large B-cell lymphoma. He was treated with an intensified chemotherapeutic course, including weekly rituximab for 10 months, and again achieved complete remission. At 11 years of age, he was found to have cervical adenopathy, and biopsy revealed large B-cell lymphoma. He had no evidence of prior EBV infection/exposure by serology, blood/tissue PCR, or *in-situ* staining of biopsy specimens. XLP was diagnosed following flow cytometric analysis of SAP, which revealed the absence of protein, as shown in Figure 1. Following re-induction of remission and confirmatory genetic testing (Table 1), he underwent unrelated bone marrow transplantation following a reduced-intensity

conditioning (RIC) regimen consisting of alemtuzumab, fludarabine, and melphalan. He is doing well > 1 year after transplant, showing full donor engraftment and immune reconstitution.

Case 2: Patient 2 (Pt2) had a distant history of large B-cell lymphoma at the age of 2 years, characterized by a paraspinal tumor, left kidney involvement, and bone marrow disease. He attained full remission after chemotherapy and paraspinal radiation. He then remained healthy until age 12 when he developed respiratory failure several weeks after varicella zoster virus (VZV) vaccine administration. CT imaging revealed bilateral infiltrates and nodules. All cultures of BAL fluid were negative, as were PCR studies including EBV, cytomegalovirus (CMV), herpes simplex virus (HSV), and VZV. *Streptococcus viridans* was identified by blood culture. The patient was noted to have hepatomegaly, bi-lineage cytopenia and a highly elevated ferritin. Splenomegaly was not noted, and bone marrow aspirate did not show hemophagocytosis. He was diagnosed with macrophage activation syndrome (MAS) and treated with methylprednisolone, cyclosporine, IVIG, and etanercept, in addition to broad-spectrum antibiotic therapy. Flow cytometric analysis of SAP expression revealed absence of protein, and genetic testing confirmed the diagnosis of XLP (Figure 1, Table 1). EBV VCA-IgM and IgG directed against EBV-Early Antigen (not transferred via IVIG) were negative. Retrospective *in-situ* staining of his original lymphoma for EBV was negative. A course of four rituximab infusions was given, followed by an unrelated donor SCT, using a RIC preparatory regimen including alemtuzumab, fludarabine, and melphalan. At >1 year post SCT, he is showing full donor engraftment and appropriate immune reconstitution.

Case 3: Patient 3 (Pt3) presented at the age of 7 years with respiratory distress and pneumonia requiring hospital admission. He later developed vomiting and seizures. Cerebrospinal fluid analyses showed mild pleocytosis and persistently elevated protein, without identifying bacterial, viral, fungal or opportunistic organisms. Brain MRI revealed bilateral mesial temporal signal abnormalities. Chest CT imaging revealed centrally located airspace disease and peripheral lung nodules, and lung biopsy showed nonspecific interstitial pneumonitis with bronchiolitis obliterans/organizing pneumonia. *In-Situ* staining and polymerase chain reaction (PCR) for EBV were negative as well. Tissue human herpesvirus 6 (HHV-6) PCR was positive. Bacterial, fungal, mycobacterial, and viral cultures were negative. A brief course of methylprednisolone therapy rapidly resolved pulmonary symptoms and abnormal CT-finding, but discontinuation led to relapse of pulmonary disease. Repeat lung biopsy again revealed interstitial pneumonitis, with a T-cell predominant lymphocytic infiltrate noted on immunohistochemical staining. All infectious studies were negative. Remission was regained with corticosteroid therapy. EBV serologies remained negative. Following diagnosis of XLP (Figure 1, Table 1), the patient received four weekly doses of rituximab. He underwent unrelated donor SCT transplantation following a RIC regimen, consisting of alemtuzumab, fludarabine, and melphalan. Now >1 year post transplant, he is showing full engraftment and early signs of immune reconstitution.

Case 4: Patient 4 (Pt4) is the 17-year old maternal half-brother of Pt3. He presented at age 9 with a large B-cell lymphoma encasing the terminal ileum. He went into remission

after completing standard-of-care lymphoma treatment and has remained otherwise healthy. EBV VCA-IgG, EBNA-IgG as well as and EBV VCA-IgM were negative, as was blood EBV PCR. Retrospective evaluation and staining of his original lymphoma tissue was negative for EBV. Following diagnosis of XLP, he was started on Rituximab and IVIG, and underwent SCT in 12/08.

Case 5: Patient 5 (Pt5) is a 31-year old man with a germline deletion of the *SH2D1A* gene, who was diagnosed after developing pancytopenia, splenomegaly, colitis and coagulopathy between 14 – 17 years of age. The patient's family history was remarkable for 3 brothers with manifestations of XLP, including pulmonary LPD, fulminant infectious mononucleosis and lymphoma. Splenectomy was performed over concerns of lymphoma. Histologic evaluation of the spleen, as well as biopsies of the bone marrow, colon and liver revealed infiltration by T and B-lymphocytes, with no evidence for malignancy or EBV infection. His symptoms all improved spontaneously following splenectomy, but stable pulmonary nodules developed over time. He developed primary EBV infection at age 25, but he responded well to treatment with Rituximab and steroids. He now has a history of chronic skin rashes akin to psoriasis, for which he receives topical treatments.

Case 6: Patient 6 (Pt6) presented at age 2 with a large multi-compartmental Burkitt lymphoma tumor emanating from the left posterolateral nasopharynx. During chemotherapy, his 2-year-old brother developed a rapidly progressive EBV infection and died within a short time. It was at this point that XLP was suspected, confirmed in Pt6 by

genetic testing. Further family history indicated that his maternal grandmother had lost 4 boys during childhood to a combination of viral illness and tumors. Genetic analysis of his 2 other brothers showed them to be normal. He is currently being scheduled for SCT.

Case 7: Patient 7 (Pt7) is the asymptomatic 2 year old brother of Pt 8 (see below), diagnosed on the basis of family history.

Case 8: Patient 8 (Pt8) is a 4-year-old boy with a history of X-linked lymphoproliferative syndrome and Burkitt's lymphoma. He was in general good health for his first 2 years of life, although he was noticed to have slow recovery from upper respiratory tract infections. In 2006 he presented with a diffuse rash and cervical lymphadenopathy. His biopsy was positive for Burkitt's lymphoma, prompting chemotherapy that brought his cancer into remission after 4 cycles. In September 2008, a chest CT showed pulmonary nodules that were diffuse and bilateral, which worsened over 2 months. A lung biopsy revealed mostly T-cell proliferation with no malignant cells. Concurrently, during this period, his brother had an episode of Burkitt's lymphoma and underwent genetic testing for XLP. Both brothers were found to have the same mutation in SH2D1A, resulting in a loss of SAP protein expression. Laboratory evaluation showed no evidence of prior EBV infection, and pan bacterial, fungal and viral cultures have all been negative to date. HHV-6 was identified by PCR in blood in 2/09, but has not been found again. He is currently being scheduled for SCT.

Supplemental Methods:

Clinical analysis of lymphocyte phenotype and function

Assays were completed in a Clinical Immunology Laboratory, in compliance with all major regulatory agencies and regulations, including CLIA, CAP, JCAHO and HIPAA. For all analyses, appropriate assay controls (healthy non-smoking subjects) were used. Results were interpreted in the context of previously obtained age-appropriate reference ranges.

Standard flow cytometry using whole blood was performed with fluorochrome-labeled mAbs to a variety of T-, B- and NK-cell markers, including CD3, CD4, CD8, CD16, CD19, CD20, CD25, CD27, CD40L, CD45, CD45RA, CD45RO, CD56, CD69, CD71, CD95, B220, inducible costimulator (ICOS), gamma/delta T-cell receptor (TCR), alpha/beta TCR, TCR-Valpha24, TCR-Vbeta11, perforin (Prf), and granzyme B (GrB). All antibodies were obtained from BD Biosciences, unless otherwise specified, and all flow cytometry was performed on a FACSCalibur or FACSCanto flow cytometer (BD Biosciences). Appropriate gating was used to define specific T- and B-cell subsets of interest. NK cells were defined by CD16 and/or CD56 expression on non-T cells. NKT cells were identified by expression of TCR-V α 24 in combination with TCR-V β 11 (obtained from Beckman Coulter) on CD3-positive lymphocytes. Determination of intracellular perforin and GrB was measured as previously described.¹⁴ In short, anticoagulated blood was first incubated with Abs detecting cell surface markers for 15 minutes at room temperature. This was followed by a standard permeabilization/fixation procedure and staining with either fluorochrome-conjugated anti-Prf or anti-GrB, or isotype-matched controls followed by washing and analysis.

Plasma levels of cytokines were measured using BioSource's Human cytokine 10-Plex kit. Samples were read on a BioRad BioPlex instrument utilizing Luminex technology. Serial dilutions of cytokine standard and normal control samples were run with each assay. Soluble levels of the alpha chain of the IL-2 receptor (sIL-2R α) were determined as previously described and compared to an established pediatric reference range.

T-cell proliferation was measured by [3 H] thymidine incorporation of peripheral blood mononuclear cells (PBMC) following incubation with mitogens phytohemagglutinin (PHA, 5 μ g/mL), concanavalin-A (ConA, 5 μ g/mL), and pokeweed mitogen (PWM, ? concentration), and/or antigens, tetanus toxoid and Candida. ICOS up-regulation was assessed by incubating whole blood for 5- and 12-hours with phorbol myristate acetate (PMA) and calcium ionophore, ionomycin.¹⁶ After the respective incubation periods, cells were labeled with fluorochrome-conjugated mAbs specific for ICOS, CD40L, and CD69 and analyzed by flow cytometry. In Pt4, concurrently with the PMA/ ionomycin experiments, whole blood was incubated with PHA (6 μ g/ml) and rIL-2 (25 U/ml) for 24 hours, followed by flow cytometric detection of ICOS, CD40L, and CD69 on CD3⁺/CD8⁻ lymphocytes.

CTL function was determined via a 2-phase cytotoxicity assay in which PBMC (effector cells) underwent a primary 7-day incubation period with irradiated (8000rad/80Gy) target cells (EBV-transformed lymphoblastic cell line [LCL]) to sensitize the effector cells. In the second phase, effector cells were incubated for 4 hours with 51 Cr-labeled LCLs at different effector/target ratios. NK-cell function was measured by incubating 51 Cr-labeled K562 target cells with PBMC. For cytotoxicity assays,

experiments were performed in triplicate, and both spontaneous (target cell lysis without the presence of effector cells) and maximum (target cells incubated in the presence of detergent to promote total cell lysis) release of ^{51}Cr were determined. Cytotoxicity for each ratio was calculated as % lysis = $[(\text{mean counts per minute [cpm] of the experiment} - \text{mean spontaneous release cpm}) / (\text{mean maximum cpm} - \text{mean spontaneous release cpm})] \times 100$ and converted into lytic units (LU).

Supplemental Table 1: Immunologic evaluations, genetic analysis, and EBV status of 4 patients seen at Cincinnati Children’s Hospital Medical Center.

	Patient 1	Patient 2	Patient 3	Patient 4
CD3+ T cells [52%-78%] / [700-4200] ^C	73% ^A / 2359 ^B	85% / 709	69% / 2732	70% / 1900
CD4+ T cells [25%-48%] / [300-2100]	44% / 1408	59% / 492	46% / 1822	48% / 1310
CD8+ T cells [9%-35%] / [200-1200]	29% / 928	26% / 217	23% / 911	20% / 546
CD19+ B cells [8%-24%] / [200-600]	17% / 556	8% / ND ^D	16% / 594	22% / 601
CD27+ B cells [14%-58%]	5.5% ^E	23%	9%	6%
CD16/56+ NK cells [6%-27%] / [70-1200]	10% / 320	15% / 125	15% / 634	7% / 191
CD8+/Prf+ T cells	ND ^F	26% ^G [$<12\%$]	16% [$<12\%$]	32% [$<28\%$]
CD8+/GrB+ T cells	ND	41% [$<31\%$]	23% [$<31\%$]	47% [$<31\%$]
PHA [> 138000]	191667 ^H	143732	143732	195926
Con-A [> 99500]	ND	ND	186788	ND
PWM [> 11600]	ND	ND	102599	ND
Candida [> 15289]	88324	95870	107801	122822
Tetanus [> 4761]	51191	11055	147970	8903
CTL [> 6]	0 ^I	0	12.9/18.1/0	1.6 / 12.1/3.3
NK-cell [> 3.1]	0.1 ^I	3.8	1.3 / 0.6/ 0.2	1.7/ 6.3 / 0.1
IgG [598-1611]	976 ^J	931	879	1046
IgM [46-263]	54	197	168	311
IgA [68-371]	28	77	177	446
Tetanus titer	Normal	ND	Poor	Poor
Diphtheria titer	Normal	ND	Poor	Poor
Pneumococcal titers	Normal	ND	Poor	Poor
Plasma IL-4 [$<119\text{pg/mL}$]	ND	$<5/76$	433/30/7	17
Plasma IL-10 [$<31\text{pg/mL}$]	ND	$<5/38$	85/21/16	<5
Plasma IFN-g [$<68\text{pg/mL}$]	ND	5/57	143/20/24	14
EBV PCR and/or <i>in situ</i> staining in tissue	Negative [lymphoma]	Negative [lymphoma]	Negative [lung]	Negative [lymphoma]
EBV PCR in fluid	Negative [blood]	Negative [blood] [BAL] ^K [CSF] ^L	Negative [blood] [CSF]	Negative [blood]
EBV VCA IgM	Negative	Negative	Negative	Negative
EBV VCA IgG	Negative	ND	Negative	Negative
EBV EBNA	Negative	ND	Negative	Negative
EBV Early Antigen	ND	Negative	ND	ND
SH2D1A analysis	Gross deletion including exons 2-4	Gross deletion including exons 1-4	195_196 insert T (A66fsX67)	195_196 insert T (A66fsX67)

A: Expressed as % of total lymphocytes

B: Expressed as # cells per microliter

C: Age-matched reference ranges

D: ND = not determined

E: Expressed as % of total B cells

F: ND = not determined

G: Expressed as % of CD8+ T cells

H: Proliferation data expressed in counts per minute (cpm)

I: CTL and NK-cell function data expressed in lytic units (LU)

J: Expressed as mg/dL

K: BAL = bronchoalveolar lavage fluid

L: CSF = cerebrospinal fluid

Supplemental Figure Legends

Supp Figure 1. Flow cytometric analysis of intracellular SAP expression.

Intracellular flow cytometry was performed on whole blood lymphocytes, gated on CD8⁺ T cells and NK cells (left panel). SAP expression was determined as a percentage of the lymphocyte subset expressing SAP in three patients and the mother of Pts 3 and 4 (Cr1=Carrier 1). SAP expression with the reference ranges of a normal control (NC) is shown for comparison.

Supp Figure 2. Cellular changes associated with RICD are blocked in XLP patients.

(A) Activated T cells from a normal control or XLP Pt 4 were restimulated with 5 µg/ml ConA or 2 µg/ml PHA. Apoptosis was measured 24 hr after treatment by PI staining and flow cytometry. (B) Activated T cells from normal controls, XLP patients, or the mother of Pts 3 & 4 (Cr1) were treated as in Figure 1 and stained with AnnexinV-FITC or DiOC₆. The % specific change (minus background) in AnnexinV⁺ cells (black bars) or DiOC₆^{lo} cells (gray bars) is shown. (C) Activated T cells were treated as in (B) and stained for intracellular, activated caspase 3. The percentage of cells positive for activated caspase 3 (black) relative to untreated (gray) is shown. (D) Activated T cells from control (C1) and Pt 5 were treated as in (B) and stained with AnnexinV-FITC or DiOC₆.

Supp Figure 3. Impaired RICD in XLP Pts 5-8. Activated T cells from a normal controls or XLP patients were cultured for 7-10 d in 100U/ml IL-2 were tested for sensitivity to apoptotic stimuli, including TCR restimulation using anti-CD3 (OKT3) mAb, agonistic anti-Fas APO1.3 mAb, staurosporine, UV-irradiation, or IL-2

withdrawal. Apoptosis was measured 24 hr after treatment by PI staining and flow cytometry. Data shown is mean \pm SD for triplicate wells, representative of two or more independent experiments.

Supp Figure 4. Naïve T cell activation in patients with XLP. (A) Peripheral blood leukocytes (PBL) were treated with 1 μ g/ml of anti-CD3 and anti-CD28 for 3 days. On day 3, blast phenotype (as assessed by forward and side scatter profile) and induction of CD25 (open histogram) on the surface of gated CD2⁺ T cells was assessed by flow cytometry compared to expression prior to activation (filled histogram). Data are representative of two independent experiments. (B) PBL were labeled with CFSE and activated with either 2 μ g/ml PHA or 1 μ g/ml OKT3 mAb plus 25 U/ml rIL-2. CD69 induction was assessed by flow cytometry 24 hr post-activation (open histogram) compared to unstimulated cells (filled histogram). CFSE dilution was measured on day 3 by flow cytometry (open histogram), compared to unstimulated cells collected on day 0 (filled histogram). (C) CD4⁺ and CD8⁺ T cells purified from fresh PBMC were stimulated with 1 μ g/ml of anti-CD3 and anti-CD28 for 3 days. On day 3, blast phenotype and CD25 induction (open histogram) was assessed by flow cytometry compared to expression prior to activation (filled histogram).

Supp Figure 5. Normal naïve T cell activation with SAP knockdown. (A) Intracellular flow cytometry for SAP expression in activated PBL 4 days post-transfection with NS- or SAP-specific siRNA. NC and XLP Pt4 cells served as positive and negative controls, respectively. (B) Naïve PBMC were transfected with NS- or SAP-specific siRNA. Viable

T cells were labeled with CFSE and activated 4 days after transfection with 1 $\mu\text{g}/\text{ml}$ OKT3 mAb plus 25U/ml IL-2. CD25 induction and CFSE dilution was measured on day 3 by flow cytometry, compared to unstimulated cells on day 0. Knockdown of SAP expression was measured by immunoblotting lysates. (B) Naïve PBMC were transfected with NS-, SAP-, or PKC-specific siRNA, then stimulated 2 days later with 1 $\mu\text{g}/\text{ml}$ of anti-CD3 and anti-CD28 mAbs. After 3 days, proliferation was measured by ^3H -thymidine incorporation (cpm). Knockdown efficiency of target proteins was measured by immunoblotting lysates.

Supp Figure 6. Silencing SAP expression attenuates RICD of EBV-specific CD8⁺ T cells. EBV-specific T cells transfected with designated siRNA were co-cultured for 24 hrs with irradiated, autologous LCL at various ratios, then stained with CD8 and AnnexinV. The percentage of viable, gated CD8⁺ T cells based on forward scatter is noted (A). The percentage of AnnexinV⁺ cells within the viable gate is noted in each histogram (B).

Supp Figure 7. Impaired induction of FASLG, BIM, and CRTAM upon TCR restimulation of XLP patient T cells. (A) Real-time PCR analysis of FASLG, BIM, and CRTAM mRNA expression in activated T cells from a normal control (NC), XLP Pts 2 & 3, and Cr1 following restimulation with 200 ng/ml OKT3 mAb for 6 hrs. Results are shown as fold induction relative to untreated cells (0 hrs), normalized to GAPDH expression at each timepoint. (B) Activated T cells were restimulated with 200 ng/ml OKT3 mAb for 24 hrs, then stained with anti-CRTAM mAb. Percentage of CRTAM⁺

cells at 24 hrs (empty histogram) versus untreated (0 hrs, filled) is noted. (C) Activated T cells were lysed following a timecourse of restimulation with 200 ng/ml OKT3 mAb. Cell lysates were separated by SDS-PAGE and immunoblotted with Abs listed at right; β -actin serves as a loading control. (D) Real-time PCR analysis of FASLG and BIM mRNA induction in activated T cells from a normal control (C1) and XLP Pt 5. (E) Immunoblotting of lysates from C1 versus XLP Pt 5 as described in (C). (F) Cells from a normal control or XLP Pt 6 were stimulated and lysed as in (C). Cell lysates were separated by SDS-PAGE and immunoblotted with Abs listed at right. (G) Activated CD4⁺ and CD8⁺ T cells from normal control (NC) versus XLP Pt 7 (purified prior to activation) were restimulated as in (C) and lysed. Cell lysates separated by SDS-PAGE were immunoblotted with Abs listed at right.

Supp Figure 8. Real-time PCR confirmation of TCR-induced genes from microarray analysis downmodulated in the absence of SAP expression. (A) NS (black) versus SAP (gray) siRNA-transfected T cells. (B) Normal control (NC, black) versus XLP Pt5 (gray) T cells. Results are shown as fold induction a 6 hrs post-restimulation with 200 ng/ml OKT3 mAb relative to untreated cells (0 hr), normalized to GAPDH expression at each timepoint.

Supp Figure 9. Knockdown of CRTAM or PD-L1 leads to a slight reduction in RICD sensitivity. Activated PBL were transfected with designated siRNA and cultured in IL-2 for an additional 4 days, then restimulated with increasing doses of OKT3 mAb. Cell death at 24 hrs was assessed by PI staining and measured by flow cytometry. Data

shown is mean \pm SD for triplicate wells.

Supp Figure 10. RNAi screen for effect of SLAM receptor silencing on TCR-induced apoptosis sensitivity. (A) Knockdown efficiency of each SLAM-R siRNA (dashed line) was measured by flow cytometry following staining with specific Abs or isotype control Abs (gray filled), relative to NS siRNA transfected cells (black line). (B) Activated T cells from a normal donor were transfected with NS- or SLAM-R-specific siRNA as designated in 3 separate experiments. Cells were restimulated with increasing doses of OKT3 mAb, and apoptosis was measured at 24 hrs by PI staining and flow cytometry. SAP siRNA transfected cells serve as a positive control.

Supp Figure 11. Silencing NTB-A expression recapitulates impaired TCR-induced target gene induction noted in SAP-deficient T cells. (A) NS (black) versus NTB-A (gray) siRNA-transfected T cells. Results are shown as fold induction a 6 hrs post-restimulation with 200 ng/ml OKT3 mAb relative to untreated cells (0 hr), normalized to GAPDH expression at each timepoint.

Supp Figure 12. CD84 is not associated with SAP in restimulated T cells. SAP was immunoprecipitated from PBL lysates prepared following a short timecourse of OKT3 stimulation. Immunoprecipitates were separated by SDS-PAGE and immunoblotted for the presence of CD84 and SAP. CD84 expression in input lysates is shown below for comparison.

Supp Figure 13. Effect of SAP on TCR-induced death is largely FYN-independent.

(A) Activated T cells were transfected with designated siRNA, cultured for 4 days, and restimulated with OKT3 mAb. Apoptosis was measured by PI staining and flow cytometry. Cell lysates prepared from siRNA-transfected cells were separated by SDS-PAGE and immunoblotted with Abs listed at right to assess knockdown efficiency of each target gene (right panel). (B) Activated XLP Pt 4 PBL were transfected with pVenus-SAP(wild-type, WT), pVenus-SAP (R78A), or pVenus alone and incubated overnight. After dead cell removal, cells were restimulated with 500 ng/ml OKT3 for 8 hrs. Apoptosis was measured by AnnexinV staining; the additional AnnexinV⁺ gate in the upper right quadrant excludes Venus⁺ cells that could not be compensated due to bright fluorescence.

Supp Figure 14. Impaired NTB-A colocalization with CD3 following restimulation in XLP T cells. Cells were stained with mAbs detecting CD3 (OKT3, green) and NTB-A (red) and left on ice (4C) or warmed to 37C for 30 min. Cells were imaged by confocal microscopy, with nuclei counterstained in blue. After deconvolution, colocalization of red and green signal (false-colored in white) was calculated using Imaris 6.2.1 software. Percentage colocalization of CD3 with NTB-A within a standard intensity threshold is shown in the 2-way histogram; axes differ based on maximum signal intensity for each sample.

Supp Figure 15. Simultaneous knockdown of SHP-1 expression partially reverses RICD resistance conferred by SAP silencing. Activated PBL were transfected with

SAP- (gray circles) or SHP-1-specific siRNA (filled squares), or both (empty squares) and restimulated with increasing doses of OKT3 mAb. Apoptosis was measured by PI staining and flow cytometry. Knockdown efficiency of SAP and SHP1 was assessed by immunoblotting (right panel).

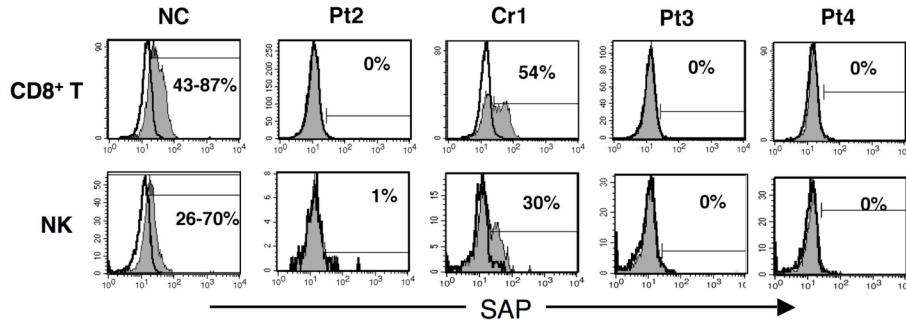
Supp Figure 16. OKT3 mAb hypercrosslinking or 64.1 mAb restores caspase activation in XLP Pt4 T cells. (A) Purified CD4⁺ and CD8⁺ T cells were restimulated with increasing doses of the anti-CD3 mAb 64.1. Apoptosis was measured by PI staining and flow cytometry. (B) Soluble FasL was measured in supernatants by ELISA from cells left untreated (untx, white bars) or restimulated with 200 ng/ml OKT3 without (gray) or with (black) 1 ug/ml Protein A, or 200 ng/ml 64.1 mAb (blue) for 8 hrs. (C) Activated PBL were treated as in (B). Caspase 8 activity was measured in prepared lysates using a colorimetric assay. (D) Cells treated with OKT3 or 64.1 mAbs as above were stained for intracellular active caspase 3 and analyzed by FACS.

Supp Figure 17. CD3 hypercrosslinking rescues FASL and BIM induction and subsequent apoptosis in XLP Pt 5 T cells. (A) Activated T cells from a normal control (NC, black) or XLP Pt5 (gray) were treated with increasing doses of OKT3 mAb in the absence (filled) or presence (empty) of 1 mg/ml Protein A, and apoptosis was measured after 24 hours. Data are representative of two or more independent experiments. (B) Cells as in (A) were lysed following 0, 4 and 8 hrs of restimulation with 200 ng/ml OKT3 mAb +/- 1 mg/ml Protein A. Cell lysates were separated by SDS-PAGE and immunoblotted with Abs listed at right. (C) Activated T cells from a normal control (NC) or XLP Pt 4

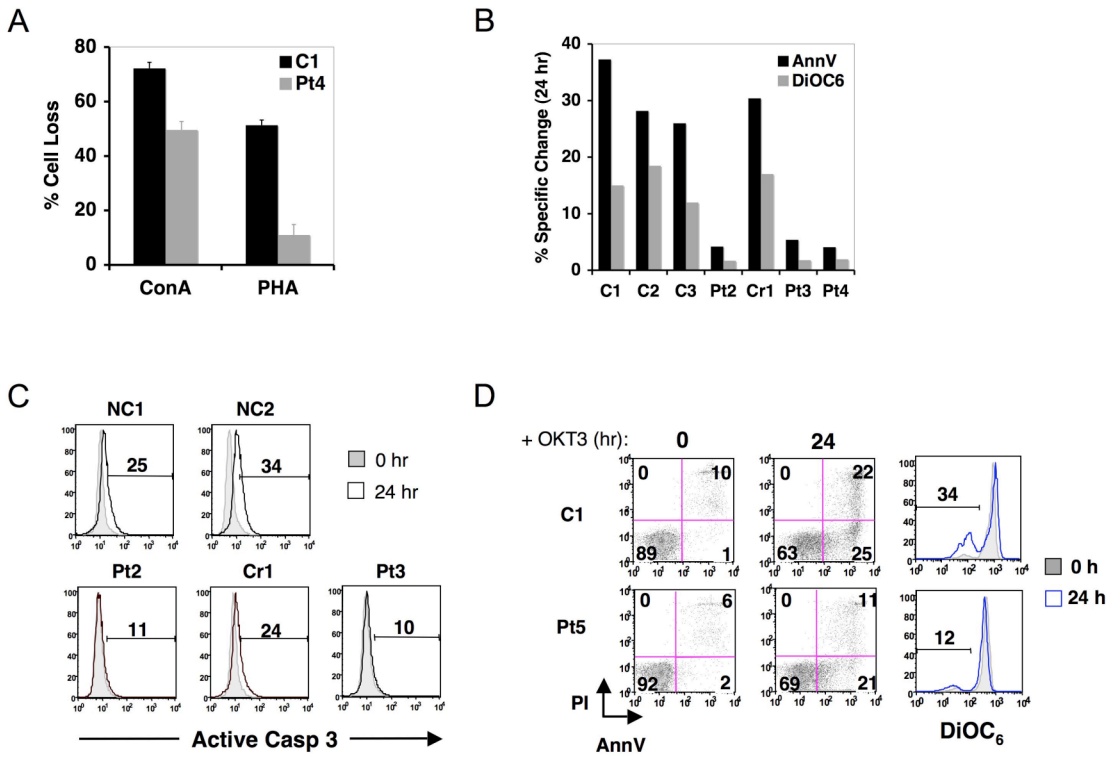
restimulated for 0 (gray filled) or 8 hrs with 200 ng/ml of OKT3 mAb in the absence (red) or presence (blue) of 1 mg/ml Protein A. Expression of CRTAM and PD-L1 was measured by flow cytometry, compared to cells stained with isotype control Abs (black).

Supp Fig 18. Analysis of AICD/p73 induction in SAP-deficient T cells. (A) CFSE-labeled PBL were treated with 1 μ g/ml of anti-CD3 and anti-CD28 for 4 days, then stained with AnnexinV-PE. The percentage of AnnexinV⁺ (apoptotic) in dividing cells is denoted in each dot plot. Alternatively, PBL transfected with NS or SAP-specific siRNA were stimulated and analyzed as above. (B) PBL were activated as above over 3 days, and p73 expression was measured in lysates made at 24 hr intervals. (C) RT-PCR quantitation of p73 and FasL expression following 6 hr restimulation of activated PBL.

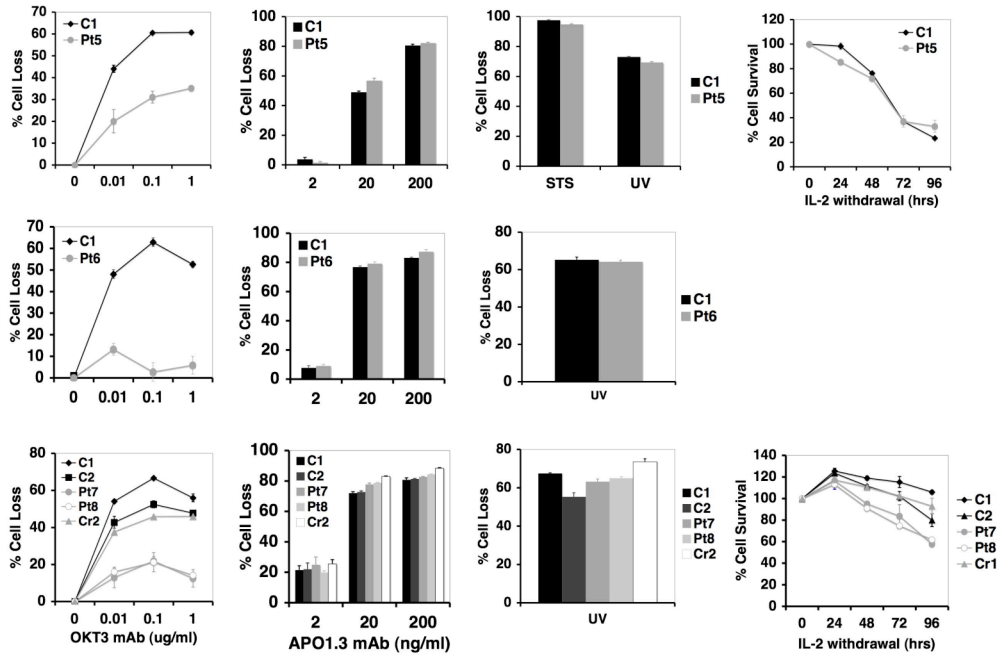
Supp Figure 1.



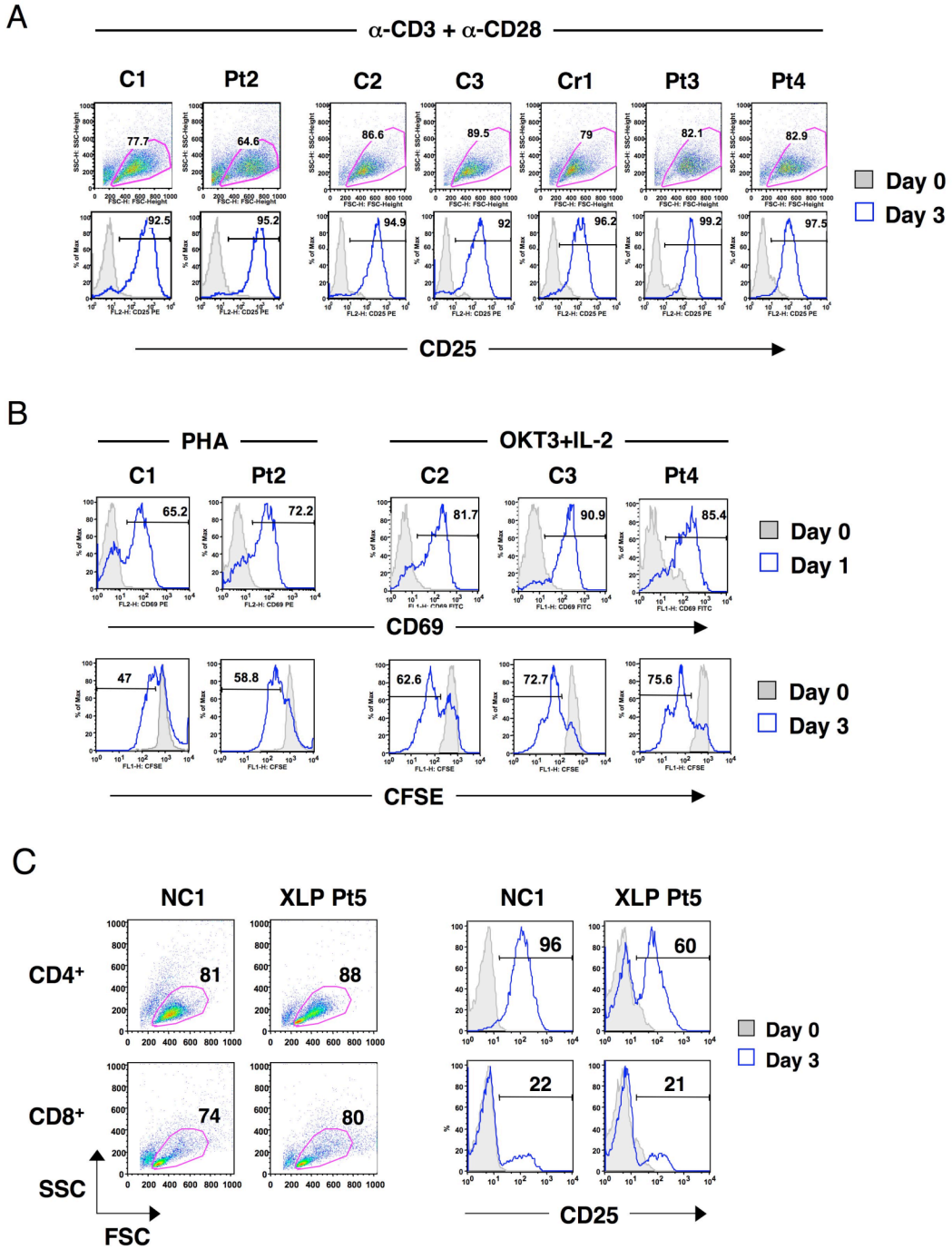
Supp Figure 2.



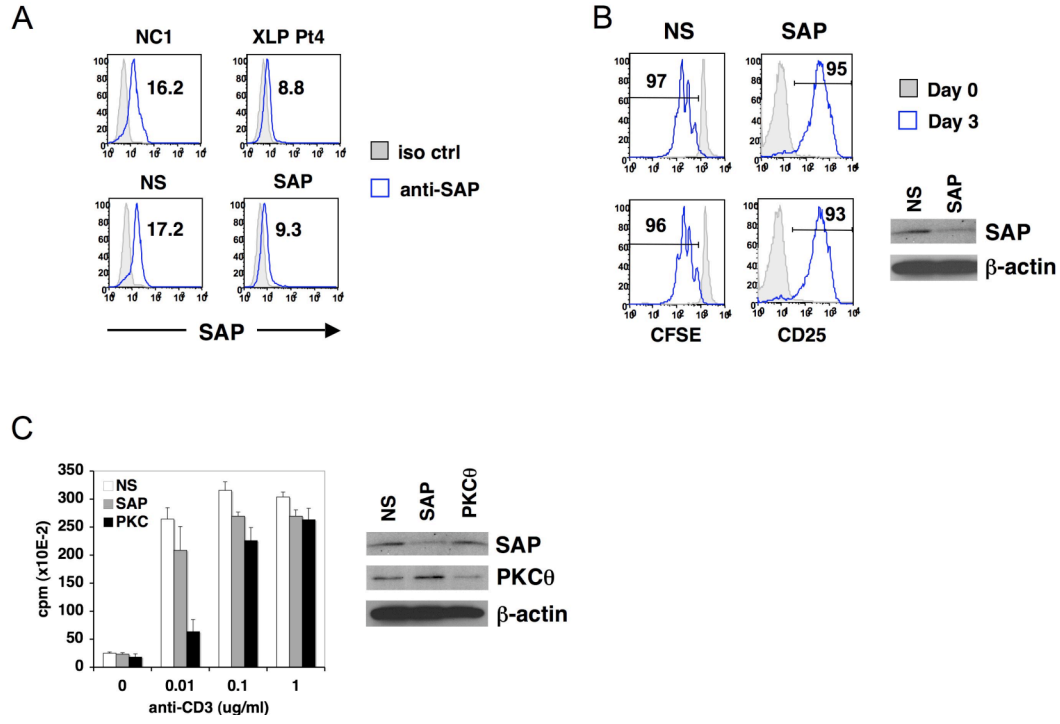
Supp Figure 3.



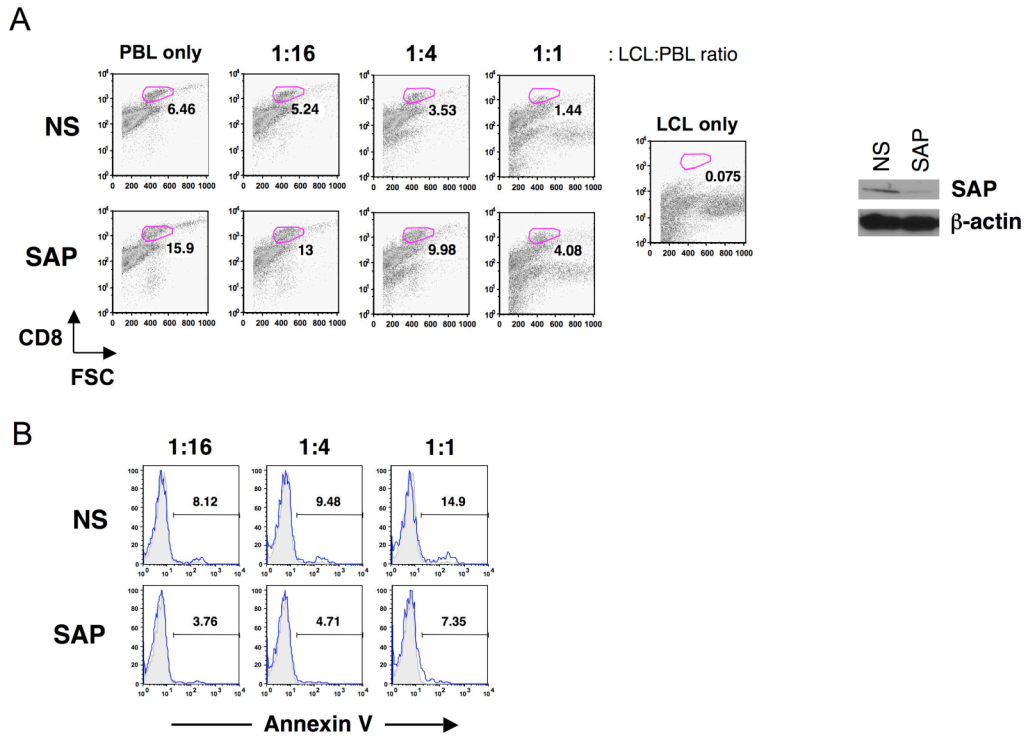
Supp Figure 4.



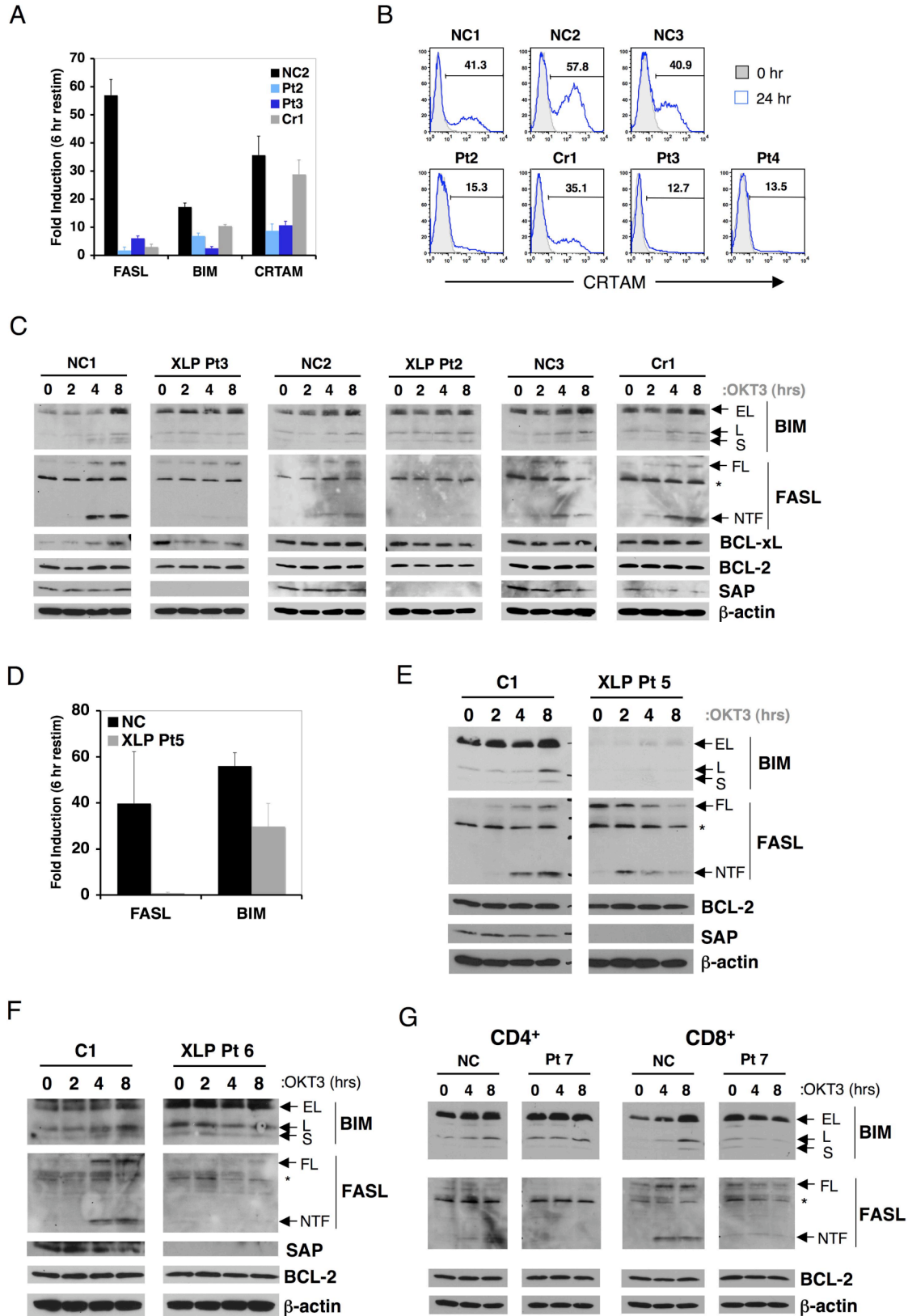
Supp Figure 5.



Supp Figure 6.

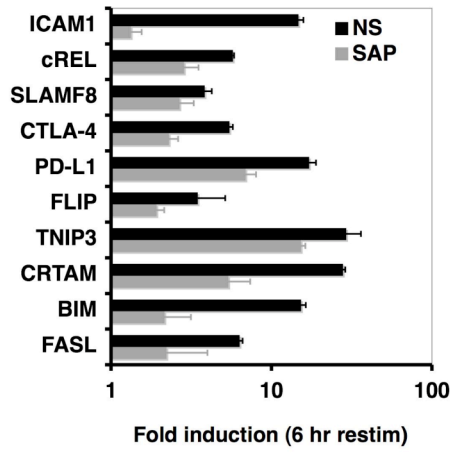


Supp Figure 7.

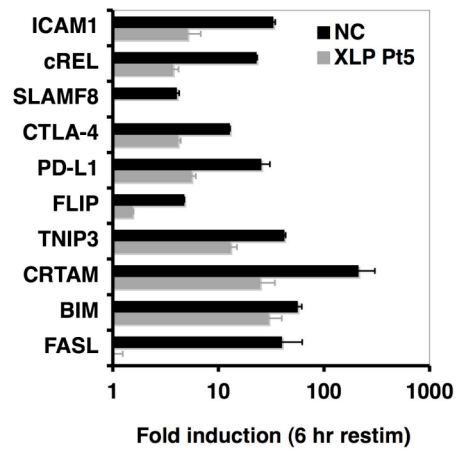


Supp Figure 8.

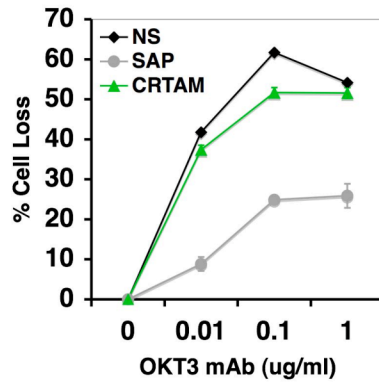
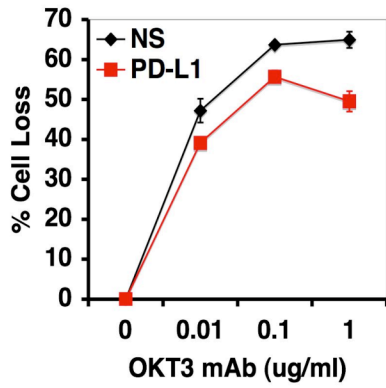
A



B

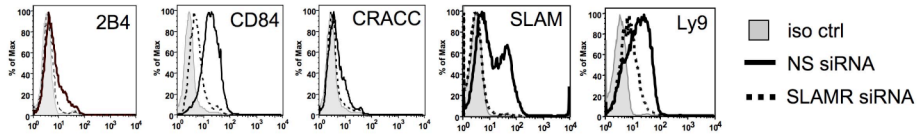


Supp Figure 9.

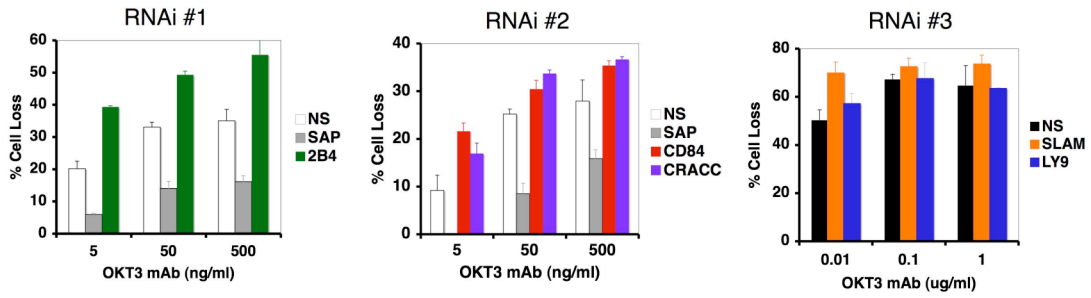


Supp Figure 10.

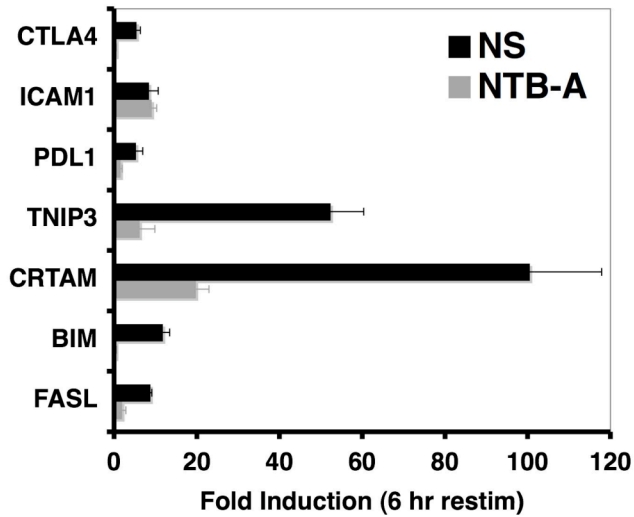
A



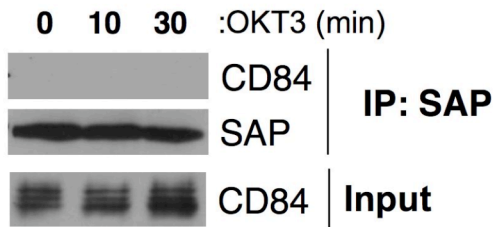
B



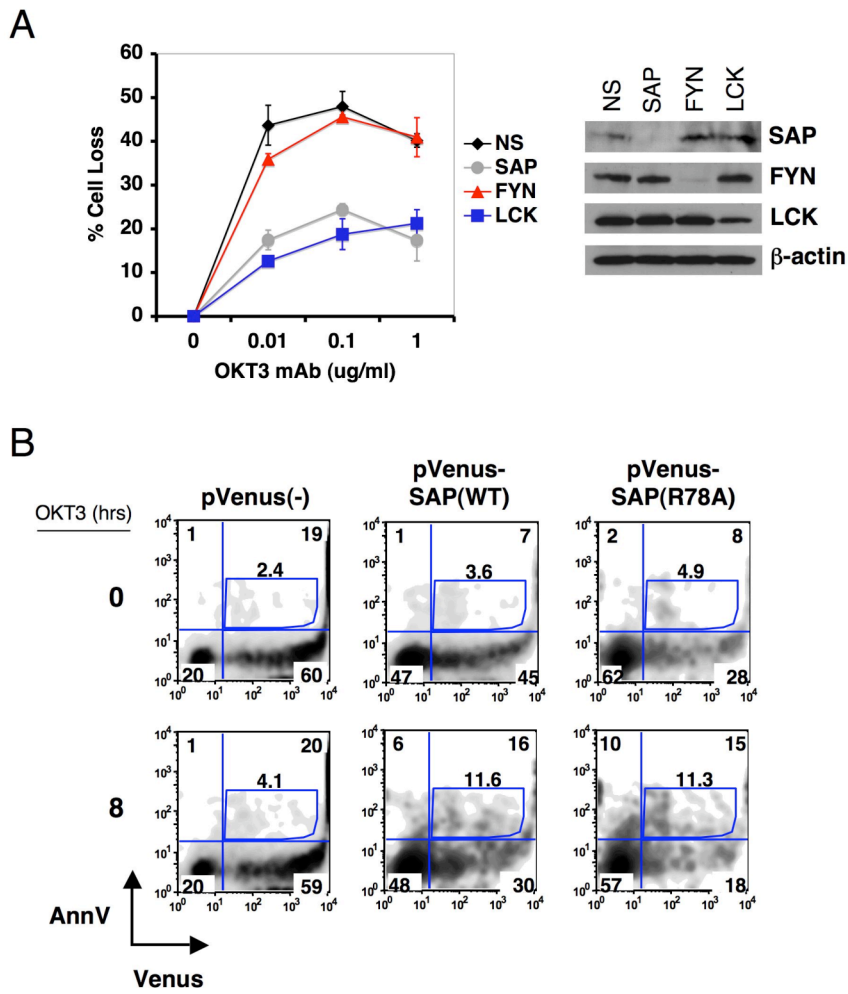
Supp Figure 11.



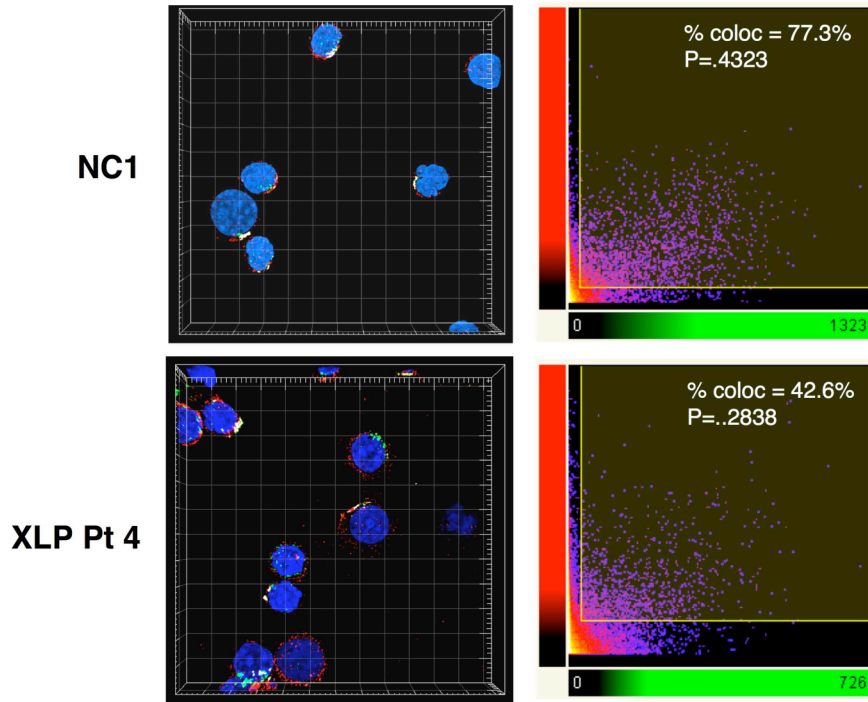
Supp Figure 12.



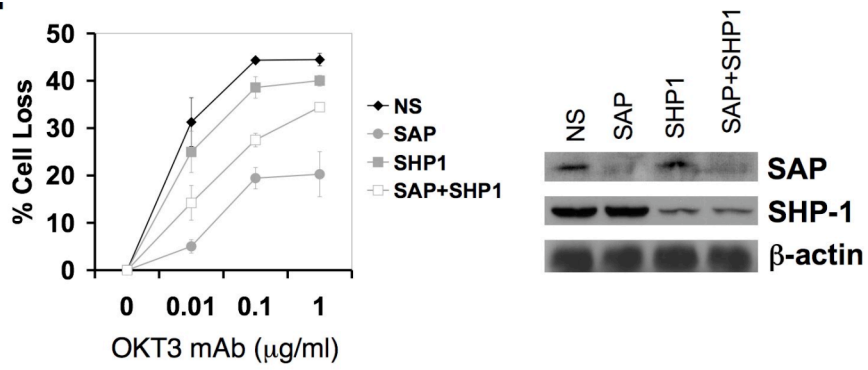
Supp Figure 13.



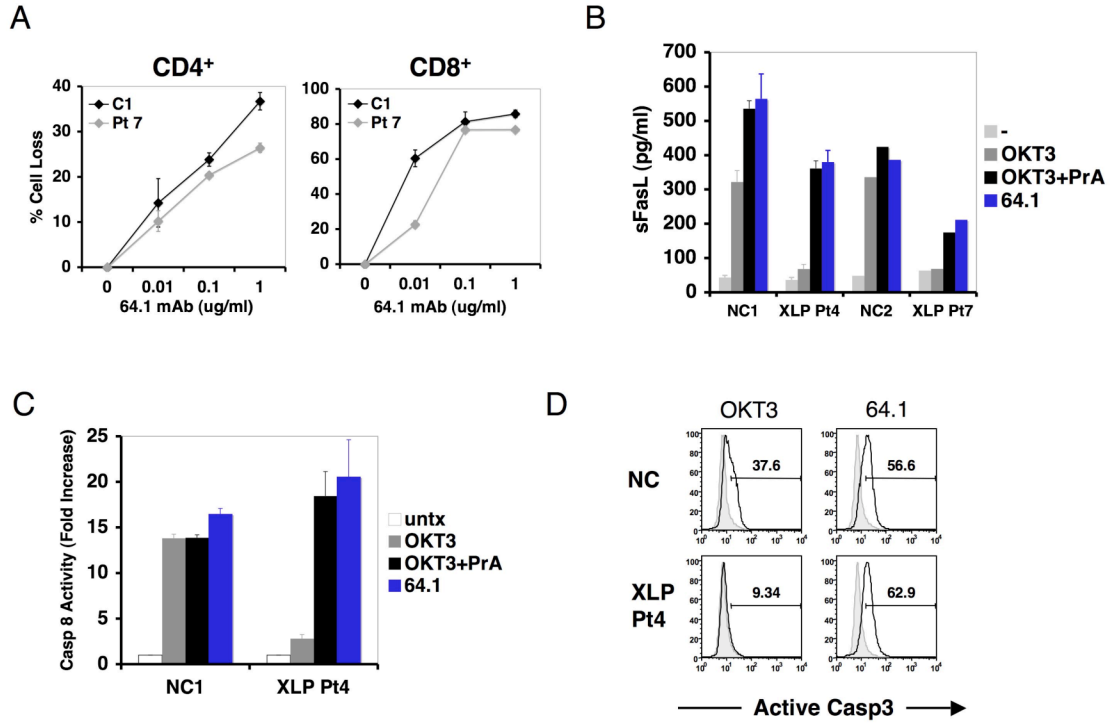
Supp Figure 14.



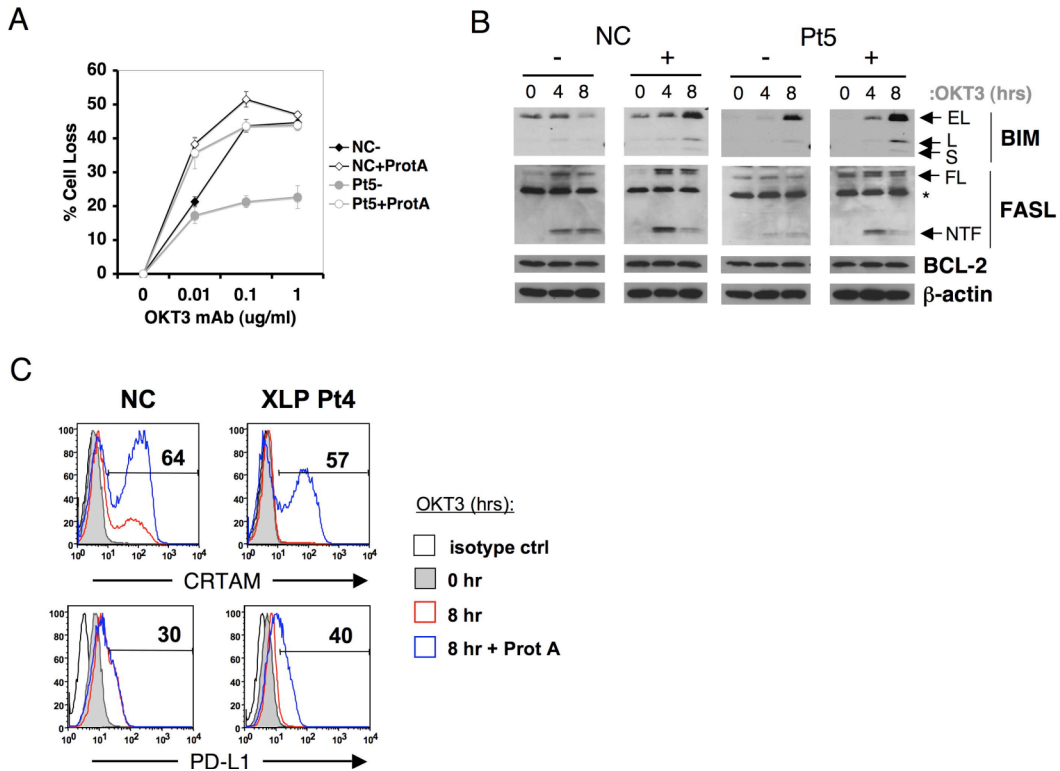
Supp Figure 15.



Supp Figure 16.

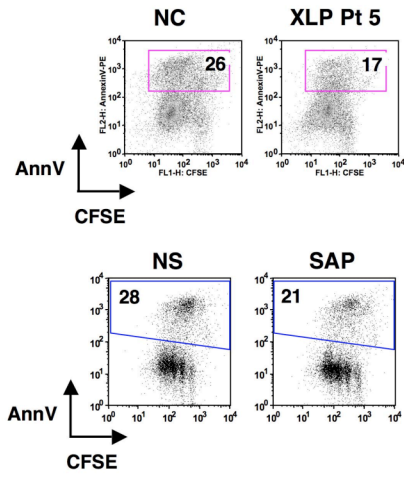


Supp Figure 17.

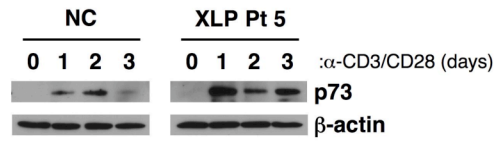


Supp Figure 18.

A



B



C

